



**HAL**  
open science

## The three-dimensional structure of the toxic peptide Cl13 from the scorpion *Centruroides limpidus*

Andrea Estefanía López-Giraldo, Timoteo Olamendi-Portugal, Lidia Riaño-Umbarila, Baltazar Becerril, Lourival D. Possani, Muriel Delepierre, Federico del Río-Portilla

### ► To cite this version:

Andrea Estefanía López-Giraldo, Timoteo Olamendi-Portugal, Lidia Riaño-Umbarila, Baltazar Becerril, Lourival D. Possani, et al.. The three-dimensional structure of the toxic peptide Cl13 from the scorpion *Centruroides limpidus*. *Toxicon*, 2020, 184, pp.158 - 166. 10.1016/j.toxicon.2020.06.011 . hal-03490267

**HAL Id: hal-03490267**

**<https://hal.science/hal-03490267>**

Submitted on 23 Jun 2022

**HAL** is a multi-disciplinary open access archive for the deposit and dissemination of scientific research documents, whether they are published or not. The documents may come from teaching and research institutions in France or abroad, or from public or private research centers.

L'archive ouverte pluridisciplinaire **HAL**, est destinée au dépôt et à la diffusion de documents scientifiques de niveau recherche, publiés ou non, émanant des établissements d'enseignement et de recherche français ou étrangers, des laboratoires publics ou privés.



Distributed under a Creative Commons Attribution - NonCommercial 4.0 International License

1

2 Title: **The three-dimensional structure of the toxic peptide C113 from the scorpion**  
3 ***Centruroides limpidus***

4

5 *Name of authors:* Andrea Estefanía López-Giraldo<sup>1</sup>, Timoteo Olamendi-Portugal<sup>2</sup>, Lidia  
6 Riaño-Umbarila<sup>2,3</sup>, Baltazar Becerril<sup>2</sup>, Lourival D. Possani<sup>2</sup>, Muriel Delepierre<sup>4\*</sup> and  
7 Federico del Río-Portilla<sup>1\*</sup>

8

9 Institutions:

10 1. Instituto de Química, Universidad Nacional Autónoma de México, Circuito Exterior s/n,  
11 Ciudad Universitaria, CdMx, 04510, México.

12 2. Instituto de Biotecnología, Universidad Nacional Autónoma de México, Av.  
13 Universidad, 2001 Colonia Chamilpa, Cuernavaca, Morelos 62210 México.

14 3. Cátedra CONACYT - Instituto de Biotecnología, Universidad Nacional Autónoma de  
15 Mexico, Av. Universidad, 2001 Colonia Chamilpa, Cuernavaca, Morelos 62210 México

16 4. CNRS UMR3528, Department of Structural Biology and Chemistry, Institut Pasteur,  
17 Paris, France.

18

19 Abstract

20 C113 is a toxin purified previously from the venom of the Mexican scorpion *Centruroides*  
21 *limpidus*. This toxin affects the function of voltage gated Na<sup>+</sup>-channels, human subtypes  
22 Nav1.4, Nav1.5 and Nav1.6 in a similar manner as other known  $\beta$ -toxins from scorpion  
23 venoms. Here, we report a correction of the primary structure of C113, previously  
24 published. The peptide does contain 66 amino acids, but residue 58 is a tryptophan and the  
25 last C-terminal amino acid is an amidated lysine, instead of arginine. The main contribution  
26 of this communication is the determination of the 3D-structure of C113, by solution NMR,  
27 showing that C113 has the classical cysteine-stabilized  $\alpha/\beta$  (CS $\alpha/\beta$ ) folding. It has a triple  
28 stranded antiparallel beta sheet commonly present in scorpion sodium channel  $\alpha$ -toxins. In  
29 addition, we report and discuss a comparison of C113 structure with two other toxins (Cn2  
30 and Css2) from scorpions of the same genus *Centruroides*, which shows important surface

---

\* To whom correspondence should be addressed

1 similarities with the structure reported here. Finally, the lack of neutralization of C113 toxin  
2 by two single-chain antibody fragments (scFvs), named LR and 10FG2, which are capable  
3 of neutralizing various toxins from Mexican scorpions, is revised. In particular, 10FG2 is  
4 capable of neutralizing toxins C111 and C112 of the same scorpion *C. limpidus*. The reasons  
5 why LR and 10FG2 are unable of neutralizing C113 toxin are discussed.

6 Keywords: NMR solution structure; scorpion toxins; sodium channels; toxin C113.

## 7 **1. Introduction**

8 Mexico is the country where a very high number of human stings by scorpions occurs  
9 (Chippaux and Goyffon, 2008). It is estimated to be close to 300,000 people stung per year  
10 (Secretaria de Salud, 2015). It also harbors the highest biodiversity of scorpion species in  
11 the world, with 289 species described until now (Santibáñez-López et al., 2015). From this  
12 number of species, only 21 are assumed to be dangerous to humans (González-Santillán  
13 and Possani, 2018). *Centruroides limpidus*, here thereafter abbreviated *C. limpidus*, is  
14 possibly the most important species in this regard, because it is extensively distributed in  
15 the states of Morelos, Guerrero, Mexico and Michoacan. The venom of this species has  
16 been extensively studied (Alagón et al., 1988; Cid-Uribe et al., 2019; Dehesa-Dávila et al.,  
17 1996; Lebreton et al., 1994; Riaño-Umbarila et al., 2013). Initially, two main toxic peptides  
18 were described C111 (Ramírez et al., 1994) and C112 (Dehesa-Dávila et al., 1996) which are  
19 capable of impairing proper function of sodium ion-channels (Possani et al., 1999). Our  
20 group is interested in developing human antibody fragments capable of protection against  
21 toxins of this scorpion and others of the genus *Centruroides* of Mexico (Riaño-Umbarila et  
22 al., 2019, 2016). Previous work by our group showed that a single-chain antibody (LR)  
23 directed against toxin Cn2 of another species of scorpion (*C. noxius*) was capable of  
24 neutralizing the entire soluble venom of this species (Riaño-Umbarila et al., 2011).  
25 Similarly, a single-chain antibody of human origin (10FG2) showed to be adequate for  
26 complete neutralization of the above mentioned toxins C111 and C112 (Riaño-Umbarila et  
27 al., 2019). Besides, a mixture of these antibody fragments was not capable of fully  
28 protecting against the entire soluble venom of *C. limpidus*, contrary to what it was shown  
29 with toxin Cn2 and the corresponding whole venom as well as some other venoms. The  
30 experimental mice injected with these two single-chain antibodies survived the challenge,

1 but still showed symptoms of intoxication. This prompted us to conduct further  
2 characterization of possible minor toxic components present in the venom of *C. limpidus*,  
3 which were not protected by our newly developed antibodies. In fact, a minor component,  
4 denominated C113 was found. It is very toxic to mice. The peptide was isolated, sequenced,  
5 physiologically characterized and published (Olamendi-Portugal et al., 2017). For the scFv  
6 10FG2 that recognizes C111 and C112, the cognate epitope on the toxins have been located.  
7 Since the amino acid sequence similarity of C113 compared to that of C111 and C112 is over  
8 70% identical, it suggests the need for further knowledge of their 3D-structures. For this  
9 reason the determination of the three-dimensional structure of C113 was undertaken. With  
10 this information, we hoped conducting comparative studies with the various scorpion toxins  
11 of the genus *Centruroides*, for which the structure and function are known. The NMR  
12 analysis of C113 indicated that a discrepancy in the reported primary structure of peptide  
13 was found. The sequence analysis by Edman degradation of the peptide was repeated with  
14 more material and the discrepancy was elucidated. The conduction of this work was very  
15 important, as we describe below, because the NMR results helped solving an ambiguity  
16 found in the primary structure of C113, as earlier published. Position 58 corresponds to a  
17 tryptophan and position 66 was identified as an amidated lysine, instead of an arginine. In  
18 addition, the determination of C113 3D-structure allowed to conduct a comparative analysis  
19 with the other known toxic peptides, which is the main contribution of this manuscript.

## 20 **2. Material and Methods**

### 21 *2.1 Source of material*

22 Scorpions of the species *C. limpidus* were collected in Iguala (latitude 17.850, longitude  
23 100.367) with official permit of SEMARNAT (number 004474/18), brought to the  
24 laboratory and milked for venom extraction. The soluble venom was fractionated, as earlier  
25 described by our group (Olamendi-Portugal et al., 2017) for obtaining purified C113. The  
26 pure peptide was used for NMR studies and *de novo* peptide sequencing.

### 27 *2.2 Amino acid sequence*

28 A PPSQ-31A Protein Sequencer from Shimadzu Scientific Instruments, Inc. (Columbia,  
29 MD, USA) was used for automatic Edman degradation. The peptide C113 was used in  
30 native and alkylated format for sequence determination. In order to obtain overlapping

1 segments of the C113 the peptide was enzymatically digested and processed as earlier  
2 described (Olamendi-Portugal et al., 2017).

### 3 *2.3 Mass spectrometry*

4 The molecular weights of toxins and peptides after digestion were obtained by mass  
5 spectrometry measurements using a LCQFleet apparatus, from Thermo Fisher Inc, (San  
6 Diego, CA, USA).

### 7 *2.4 NMR procedures*

8 NMR experiments were recorded on an either 800 MHz Avance NEO (Bruker Biospin,  
9 Billerica, MA, USA) spectrometer with an 18.1 Tesla magnetic field or a 600MHz Avance  
10 III HD spectrometer with a 14.1 Tesla magnetic field. The two spectrometers were  
11 equipped with a cryogenically cooled triple resonance  $^1\text{H}[^{13}\text{C}/^{15}\text{N}]$  probe. Spectra were  
12 recorded using TOPSPIN 4.05 (Bruker Biospin). The lyophilized toxin (about 4 mg) was  
13 dissolved in 180  $\mu\text{l}$  of 10% D<sub>2</sub>O 20 mM acetate pH 5 buffer (Euriso-Top, Saclay, France)  
14 to produce a 2.8 mM (7846 MW) sample that was studied by NMR using a 3 mm Shigemi  
15 tube (Shigemi, Alison Park, PA, USA). Experiments were run at 283, 288, 298, 303, 313  
16 and 318 K with either a 9615 Hz or 7194 Hz sweep widths. Spectra were referenced to  
17 external DSS (4,4-dimethyl-4-silapentane-1-sulfonic acid). The 2D proton NMR spectra  
18 were collected with 4 K data points in the t<sub>2</sub> dimension and 512 or 1024 t<sub>1</sub> increments,  
19 with typically 32-64 scans per increment. For spin system identification and sequential  
20 assignment, the following 2D NMR homonuclear experiments were recorded: (a) total  
21 correlation spectroscopy or Clean TOCSY (Griesinger et al., 1988) using a MLEV-17 pulse  
22 scheme with 80 ms or 40 ms isotropic mixing period (Bax and Davis, 1985; Levitt et al.,  
23 1982), (b) double-quantum spectroscopy (DQCOSY) (Wagner and Zuiderweg, 1983), (c)  
24 double-quantum filtered COSY (DQFCOSY) (Piantini et al., 1982; Rance et al., 1983) and  
25 (d) nuclear Overhauser effect spectra (NOESY) (States et al., 1982). NOESY spectra were  
26 acquired with mixing times of 100, 150 and 250 ms. Water suppression was achieved either  
27 by pre-saturation during the recycle delay or, in the NOESY experiment, by double pulsed-  
28 field gradient spin echoes (DPFGSE) (Dalvit et al., 1991; Hwang and Shaka, 1995).  
29 Assignment of signals to peptide protons was achieved by the standard method developed

1 by Wüthrich (Wüthrich, 1986). HN-H $\alpha$  coupling constants were measured using the  
2 modified J-doubling method in the frequency domain (Delrioportilla et al., 1994; Garza-  
3 García et al., 2001) from 2D-TOCSY at 303 K traces. To satisfy the J-doubling method  
4 requirement, TOCSY experiment was re-transformed using 1024 X 65,536 complex points  
5 to have a resolution of 0.20 Hz / point for each trace used.

6 In addition, two dimensional heteronuclear experiments were run at 308K on the 800 MHz,  
7 namely  $^{15}\text{N}$  HSQC, Multiplicity edited  $^{13}\text{C}$  HSQC,  $^{13}\text{C}$  HSQC-TOCSY and  $^{13}\text{C}$  HMBC, to  
8 back up the proton assignments (Medvedeva et al., 1993).  $^{13}\text{C}$  and  $^{15}\text{N}$  chemical shift  
9 assignments were used to obtain Phi and Psi angles using the TalosN web server (Shen and  
10 Bax, 2013).

### 11 *2.5 Structural calculation*

12 A homonuclear  $^1\text{H}$ - $^1\text{H}$  NOESY spectrum acquired at 308 K with a 150 ms mixing time  
13 was used to obtain distance constraints for structure calculations. The experimental results  
14 obtained by NMR were processed with the software nmrPipe (Delaglio et al., 1995). CARA  
15 1.5 (Keller, 2004) software was used for spin system identification, peak picking and NOE  
16 derived distance constraints assignments. The structural calculation was run using CYANA  
17 2.1 (Downing and Güntert, 2004) with chemical shift tolerance between 0.02 and 0.015  
18 ppm. The 20 protein's models with the lowest energy values and without violations were  
19 selected between 500 structures. Additionally, 20 models with the lowest energy values  
20 were minimized and refined using molecular dynamic calculations with AMBER 9, the  
21 protocol applied was as described by Gurrola (Gurrola et al., 2012). The refined structural  
22 model of the toxin Cl13 was validated and deposited in the Protein Data Bank (PDB:  
23 6VXW). Structures were analyzed and visualized with UCSF Chimera (Pettersen EF,  
24 Goddard TD, Huang CC, Couch GS, Greenblatt DM, Meng EC, 2004).

25

## 26 **3. Results**

### 27 *3.1 Extraction and sequence*

28 Due to the ambiguity found between the earlier published amino acid sequence  
29 regarding position 58 of the primary structure of Cl13, it was decided to purify a greater

1 amount of toxin and repeat the determination of the Edman degradation. For the sequence  
2 reported in Olamendi-Portugal (Olamendi-Portugal et al., 2017), we used 75  $\mu\text{g}$  of purified  
3 C113; for the present communication we used 250  $\mu\text{g}$ . The C-terminal fragment obtained by  
4 digesting the peptide with Asp-N endopeptidase allowed determining the full sequence  
5 from residue number 53 to 66. To our surprise the last residue was lysine, instead of  
6 arginine, as earlier surmised based on mass spectrometry results. The first time the  
7 sequence was obtained by Edman degradation did not allow the identification of residue in  
8 position 66. The molecular mass obtained from the purified peptides of the C-terminal  
9 segments Glu53 to Lys66 was 1723.5 Da (see Olamendi-Portugal et al., 2017) and under  
10 the repeated experiment reported here is 1722.9 Da, which within the experimental error of  
11 our mass spectrometer means that it corresponds to the same molecular weight. These  
12 results agree with the expected molecular mass of the peptide found. It is important to  
13 mention that this C-terminal peptide had the cysteine reduced and alkylated. Knowing that  
14 the last residue was an amidated Lys66 and that in position 58 there was Trp, as shown on  
15 the NMR results, the fully corrected amino acid sequence of C113 was obtained. The  
16 molecular mass experimentally observed is (7846.6) and the expected molecular mass for  
17 the newly determined sequence is (7846.0), thus confirming the right amino acid sequence  
18 of C113.

### 19 *3.2 NMR assignments and structure calculations*

20 The sequence specific assignment of C113 were acquired according to a standard  
21 procedure (Wüthrich, 1986) using spectra recorded at different temperatures ranging from  
22 283 to 313 K to solve ambiguities due to overlapping signals. Although, linewidths of  
23 amide resonances are quite broad at 283 K for all the amide protons those sharpened up  
24 differentially when increasing the temperature the ultimate case being Phe44 amide proton  
25 only detectable at 313 K. Briefly, spin systems of all amino acid residues were identified  
26 via their through-bond connectivities observed in DQFCOSY, TOCSY and DQCOSY  
27 whereas sequential assignments were obtained using the through space connectivities ( $\text{NH}_i$ -  
28  $\text{NH}_{i+1}$ ,  $\text{H}\alpha_i$ - $\text{NH}_{i+1}$  and  $\text{H}\beta_i$ - $\text{NH}_{i+1}$ ) observed between neighboring residues in the NOESY  
29 spectra. While fairly strong NOEs sequential interactions were observed between the  $\text{H}\alpha$   
30 proton of Leu60 and the  $\text{H}\delta$  of Pro61 allowing to assign the *trans* conformation for the  
31 Leu60-Pro61 peptide bond. Although unambiguous NOE sequential interaction could not

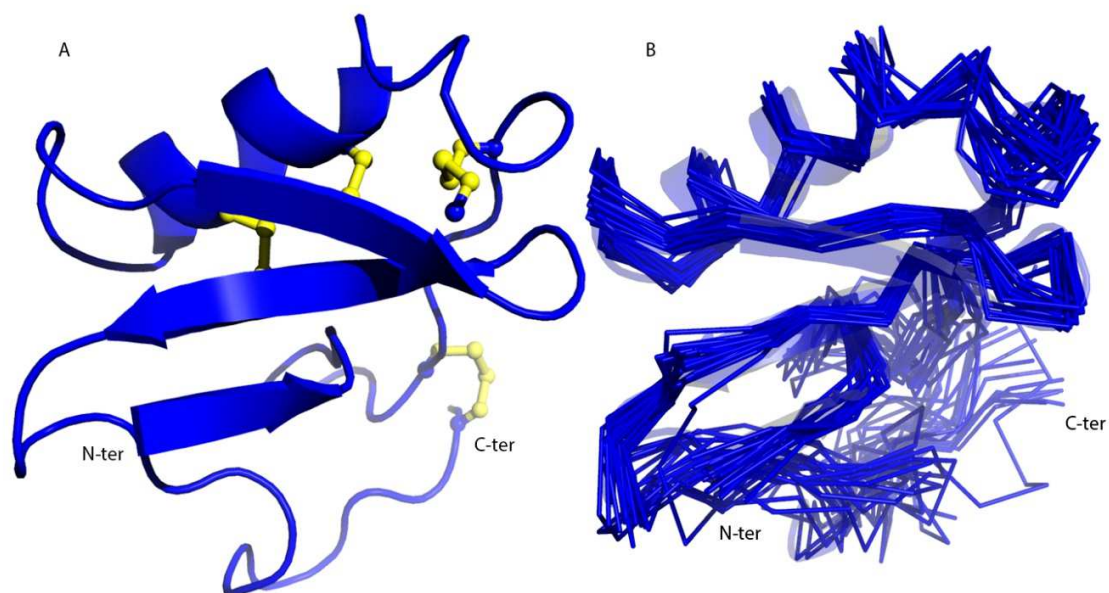
1 be stated between the H $\alpha$  protons of Trp58 and Pro59 as a result of unfortunate overlap  
2 between Phe44 H $\alpha$  and H $\beta$  protons with Trp58H $\alpha$  and Pro59 H $\alpha$  protons respectively, the  
3 up-field shifted value of the Pro59 H $\alpha$  chemical shift, 3.62 ppm together with the lack of  
4 NOE interaction between Trp58 H $\alpha$  and Pro59 H $\delta$  protons are in favor of a Trp58-Pro59  
5 peptide bond in the *cis* conformation (Dyson et al., 1988).

6 To complete the proton assignments 2D  $^{13}\text{C}$ - $^1\text{H}$  HSQC, HSQC-TOCSY and HMBC were  
7 acquired using the natural unlabeled protein. The carbon chemical shifts displayed  
8 characteristic ranges for each amino acid providing sufficient information to back up the  
9 proton assignments. The  $^{13}\text{C}$ -HSQC with multiplicity editing was of significant importance  
10 because it allowed direct identification of Gly H $\alpha$  protons, Val, Ser and Thr H $\beta$  protons.  
11 The  $^{13}\text{C}$ - $^1\text{H}$  HSQC-TOCSY was quite helpful to complete side chain assignments of Pro,  
12 Lys, Arg whereas the HMBC was used to complete carbon signals of aromatic side chains  
13 (Medvedeva et al., 1993).

14 The C113 HN-H $\alpha$  coupling constants, proton, carbon and nitrogen chemical shifts are  
15 deposited in the Biological Magnetic Resonance Bank (BMRB: 30727). The 150 ms  
16 mixing time NOESY and 80 ms TOCSY at 308 K spectra showed a reasonable signal  
17 dispersion which allowed identifying the 66 spin systems of all amino acid residues;  
18 however, the dispersion was not good enough to measure H $\alpha$ -H $\beta$  coupling constants. The  
19  $^1\text{H}$ ,  $^{13}\text{C}$  and  $^{15}\text{N}$  completeness assignment are 93%, 66% and 72% respectively at natural  
20 abundance sample used. The solution structure of C113 (Figure 1) was obtained from 2,102  
21 NOEs with off diagonal assignment; 253 of them are long-range NOEs  $|i-j| \geq 5$ , 132  
22 medium-range NOEs  $1 < |i-j| < 5$  and 1,717 short-range NOEs  $|i-j| \leq 1$  (Figure 2), 67 angle  
23 restrictions from TalosN and 48 HN-H $\alpha$  coupling constants. Figure 1A shows the C113  
24 NMR solution structures, which comprise an  $\alpha$ -helix (Tyr24-Arg32), a triple stranded  
25 antiparallel  $\beta$ -sheet (Lys1-Tyr4, Ala45-Leu51 and His38-Tyr42), three loops ( $\beta$ 1- $\alpha$ 1,  $\alpha$ 1- $\beta$ 2  
26 and  $\beta$ 2- $\beta$ 3) and four disulfide bridges. Figure 1B shows the superposition of the 20 lowest  
27 energy structures. The final average backbone RMSD to mean was 0.66 and considering  
28 the heavy atoms RMSD to mean was 1.04. A summary of the experimental constraints and  
29 structure calculation statistics are shown in Supplementary Material Table S1. Temperature  
30 coefficients of amide proton as a function of temperature were measured from 10°C to



1 45°C (1D spectra are shown in the Supplementary Material Figure S1). The sample in H<sub>2</sub>O  
2 was freeze dried and dissolved in D<sub>2</sub>O to assign the remaining amide assuming they are  
3 hydrogen bonded.



4  
5 Figure 1. A) NMR solution structure of C113 with the lowest energy. The disulfides are  
6 painted in yellow. B) Backbone superposition of the 20 lowest energy structures of C113.  
7 The C-terminus is amidated. Structure calculation without disulfide bonds and  
8 superposition of the C113 with and without disulfide bond restrictions are in Supplementary  
9 Material Figure S2-3 respectively.

10



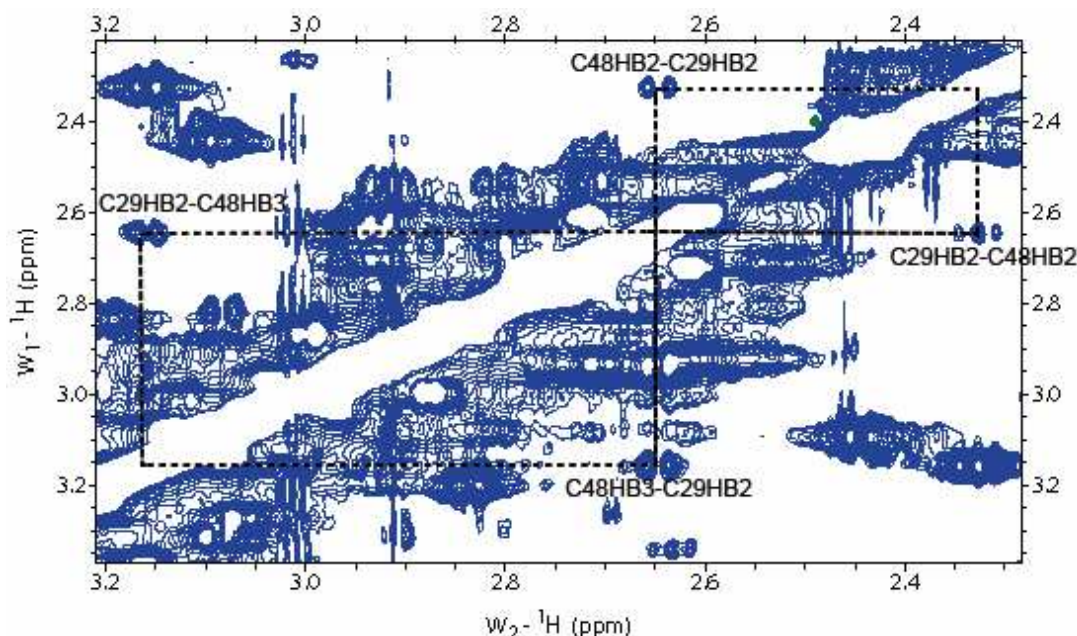
1

2 Figure 2. NOE's used in the structure calculations. Thick, medium and thin lines  
 3 correspond to short, medium and long range NOE's. It could be seen clearly the  $\alpha$ -helix in  
 4 between residues Asp23-Tyr33, a double  $\beta$ -stranded antiparallel  $\beta$ -sheet (His38-Tyr42 and  
 5 Ala45-Leu49). The  $\beta$ -strand between Glu2-Leu5 is hardly seen; however, the angle  
 6 measurement and proximity found with the second  $\beta$ -strand shows its existence. NMR  
 7 statistics and Ramachandran plot are in Supplementary Material Figure S4.

8

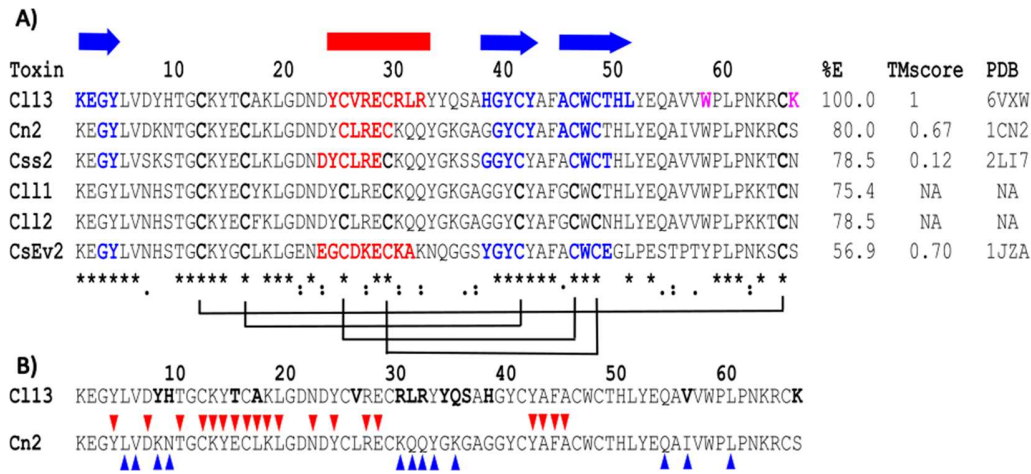
9 We performed two different structure calculations to define the disulfide bonds: the first  
 10 one, without S-S bond constraint; and, the second one with S-S bonds (C1-C8, C2-C5,  
 11 C3-C6, and C4-C7) relative to the primary structure. The two calculations converged to  
 12 very similar structures, see Figure S-2. The S-S bonds used for the second calculation were  
 13 those observed by NMR. Indeed, NOE's were clearly observed between  $H\beta_i$ - $H\beta_j$  and  $H\alpha_i$ -  
 14  $H\beta_j$  of the cysteines present in each disulfide bond. We present the Cys29 $H\beta$  and-Cys48  $H\beta$   
 15 NOE correlation in Figure 3. It can be seen that no overlap can hinder the interpretation.  
 16 These calculations and the NOE's indicate that the specific cysteines are close by and  
 17 therefore should be forming a bond between them. Also, the other  $H\beta$  regions (Cys16-  
 18 Cys41, Cys25-Cys46 and Cys65-Cys12) can be observed in Figure S-3.  $H\alpha/H\alpha$ ,  $H\alpha/H\beta$   
 19 NOEs between C41 and C46, which are not covalently linked each other, were also

1 observed as a result of beta strand formation. Considering these two results and the fact that  
2 this disulfide bond arrangement is similar to all other  $\beta$ -toxin whose structures are known,  
3 we added those restrictions to the calculation.

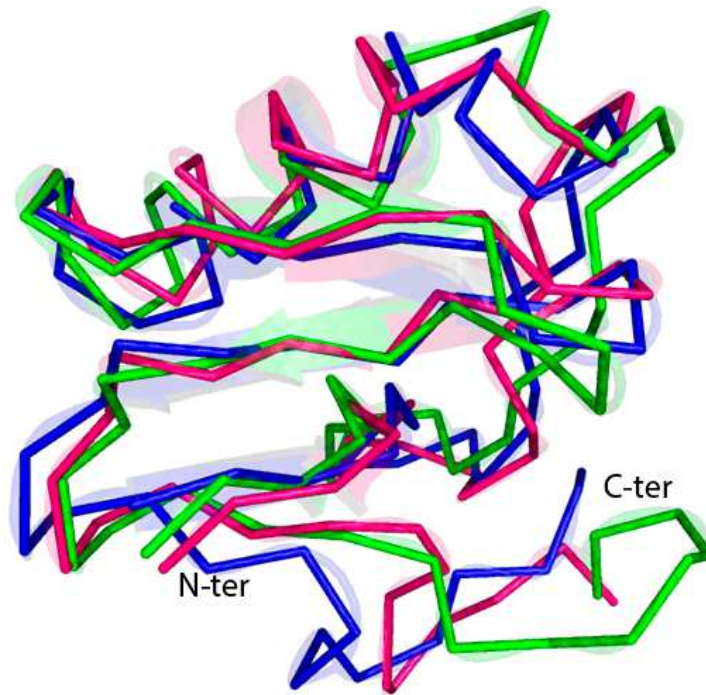


4  
5 Figure 3. H $\beta$ -H $\beta$  region of Cys29-Cys48 2D NOESY disulfide correlation obtained for  
6 C113 experiment at 150 ms mixing time, 308 K, pH5 and 2.8 mM toxin concentration;  
7 assignments are labeled in black. The whole NOE correlation regions of cysteines forming  
8 disulfide bonds are in the Supplementary Material Figure S3. It can be seen that those  
9 correlations are well defined. This figure was made with NMRFAM-SPARKY software  
10 (Lee et al., 2015).

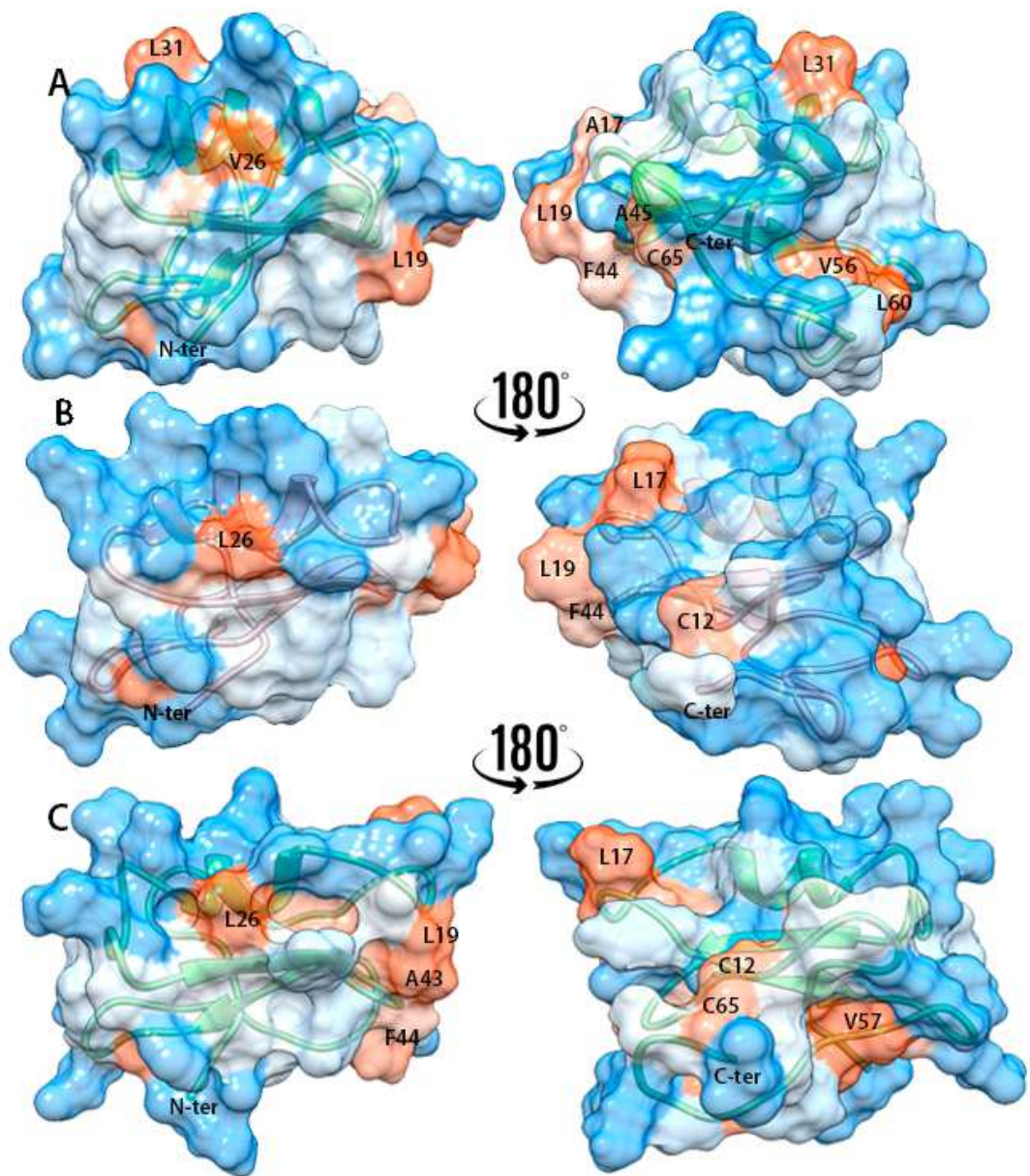
11  
12 Figure 4 shows the sequence alignment of C111, C112, C113, Cn2, Ccss2 and Csev2 toxins  
13 which have high identity percentage and tertiary structures reported in the PDB for C113,  
14 Cn2, Ccss2 and Csev2 toxins only. The amino acids that form  $\beta$ -strands are highlighted in  
15 blue meanwhile those that form  $\alpha$ -helices are highlighted in red. The differences found in  
16 the secondary structure elements are highlighted in Figure 4. Additionally, C113 shows a  
17 well defined first  $\beta$ -strand. Figure 5 shows Cn2, Ccss2 and C113 backbone superposition of  
18 their structures. All of these toxins have a CS $\alpha$  $\beta$  folding motif.



1  
2  
3 Figure 4. A) Sequence alignment of beta toxins C113, Cn2, Css2, C111, C112 and CsEv2.  
4 The two amino acids corrected of C113, Trp58 and Lys66, are colored in pink. The  $\beta$ -sheet  
5 region is colored in blue and the  $\alpha$ -helix in red. Disulfide bonds are marked as C1-C8, C2-  
6 C5, C3-C6 and C4-C7. The corrected residues in toxin C113 are colored in magenta.  
7 Secondary structures were determined via Chimera software. C111 and C112 do not have  
8 their 3D structures reported yet. The asterisk (\*), colon (:), and dot (.) indicate identical  
9 amino acid residues, conserved substitution, and semi-conserved substitutions in all  
10 sequences used in the alignment, respectively. Below, it is shown the disulfide bonds  
11 connectivity. This alignment was made with the server T-coffee (Notredame C, Higgins  
12 DG, 2000). %E is the identity percentage value considering exact match between amino  
13 acids. The TM score (Xu and Zhang, 2010) compares 3D structures, it is convenient to  
14 consider not only the sequences alignments, but also 3D structures to see their similarities.  
15 TM score makes this comparison and produces a number between 0 and 1. The value is 0  
16 when they do not match. The value is 1 if they match perfectly. B) Sequence alignment of  
17 Cn2 and C113 highlights the amino acid residues recognized in Cn2 by scFv LR in red  
18 triangles and the ones recognized by scFv 10FG2 in blue triangles. Differences between  
19 aminoacids C113 and Cn2 are highlighted in bold.

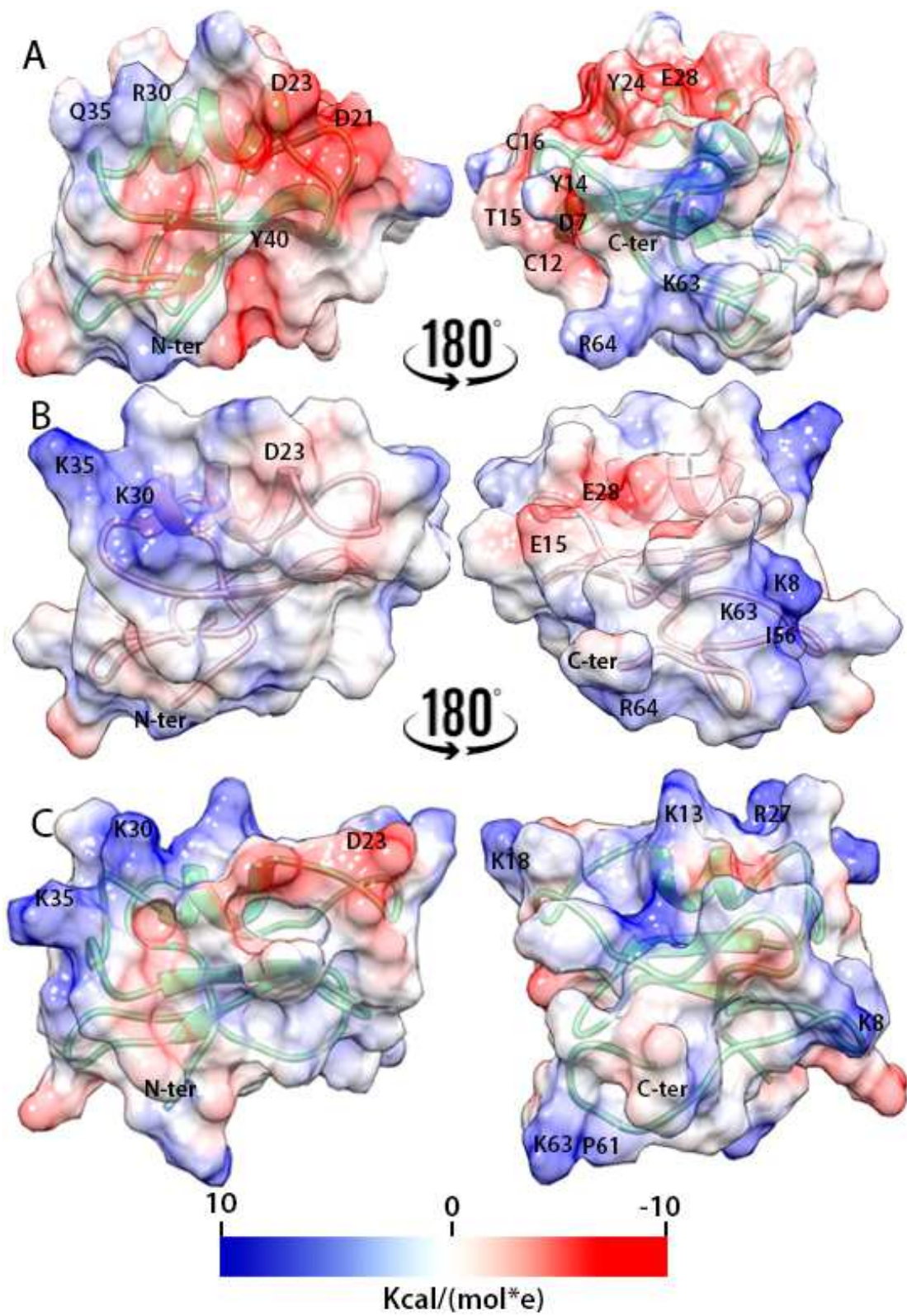


1  
2 Figure 5. Structure comparison between Cn2 (pink), Ccss2 (green) and C113 (blue) where  
3 can be observed that all these toxins have similar structure. We have eliminated the His tag  
4 for Ccss2. Differences in activity should be due to specific amino acid positions.  
5  
6 The structures being established, we did calculate the hydrophobic (figure 6) and the  
7 coulombic (figure 7) regions of C113, as well as those of Ccss2 of *Centruroides suffusus*  
8 *suffusus* (Saucedo et al., 2012) and Cn2 of *Centruroides noxius Hoffmann* (Pintar et al.,  
9 1999), as these are highly similar in activity and have their 3D structure solved in order to  
10 contrast those regions which have been relevant for the toxin function.



1  
2  
3  
4  
5  
6  
7

Figure 6. The hydrophobic surfaces were calculated using UCSF Chimera (Pettersen EF, Goddard TD, Huang CC, Couch GS, Greenblatt DM, Meng EC, 2004) of the toxins A) Cl13, B) Css2 and C) Cn2. The surfaces were colored according to a scale of three colors where blue indicates a polar region, white a neutral region and orange a hydrophobic region.



1 Figure 7. Comparison between the coulombic surfaces of A) Cl13 and B) Cn2 and C) Css2.  
2 Positively charged regions are in blue, negatively charged regions are in red. We use UCSF  
3 Chimera software (Pettersen EF, Goddard TD, Huang CC, Couch GS, Greenblatt DM,  
4 Meng EC, 2004) to create this figure.

#### 5 **4. Discussion**

6 Cid-Uribe et al. (Cid-Uribe et al., 2019) in their recent published transcriptomic analysis  
7 of venom components from *C. limpidus* reported the presence of a gene that possibly codes  
8 for the toxin Cl13. The authors report the identification of 59 transcripts with similar amino  
9 acid sequence as those described for known Na<sup>+</sup>-channel specific toxins. One of them  
10 (CLiNaTbet37, C0HK69) was exactly the same as the sequence now corrected for Cl13.

11 Taking into account the high sequence homology with two other beta-scorpion toxins Css2  
12 of *Centruroides suffusus suffusus* (Saucedo et al., 2012) and Cn2 of *Centruroides noxius*  
13 *Hoffmann* (Pintar et al., 1999) whose structures have been solved by our teams, we used the  
14 two NMR experimental beta-scorpion toxin structures in order to compare them with the  
15 resulting structure of Cl13 (Figure 1A). Indeed, all of them are toxic to mammals; however,  
16 while Cl13 and Css2 have a strong activity over hNav1.5 channel (Olamendi-Portugal et  
17 al., 2017; Schiavon et al., 2006), Cn2 has a strong activity over hNav1.6 channel. An  
18 intrinsic property of toxin Cl13 is that although it also affects hNav 1.6 channels it displays  
19 some interesting and unusual effects on the inactivation process.

20 The sequence identity of the toxins shown in Figure 4 is higher than 56% (78% with Cn2  
21 and 56.9% with Css2). The 3D structures differed in limited regions, see Figures 3-6.  
22 Indeed, sequence alignment of Cl13, Cn2, Css2 and CsEv2 toxins shows a high identity  
23 percentage which correlates with their conserved tertiary structures reported in the PDB  
24 sharing the typical CS $\alpha$ / $\beta$  folding. The TM score is 0.67 for Cn2 and Cl13, indicating that  
25 there is a good match between these two structures (see Figure 4). The differences between  
26 these toxins are only in the length of amino acid segments which form the secondary  
27 structure elements. However, the alignment between Cl13 and Css2 produces very different  
28 results because there is some extra amino acids present in Css2 which give a small TM  
29 score value; nevertheless, these two structures are very similar considering visual  
30 comparison (Figure 5). It is interesting to note that the first  $\beta$ -strand in Cl13 involving



1 residues 2 to 4 while for Cn2 and Css2 only two amino acids are involved. We are thus  
2 expecting that binding differences are due to exposed amino acids which results in the lack  
3 of antibody recognition. Glu15 in Cn2 was replaced with Thr15 in C113 which is exposed  
4 (Figure 4.B, 6 and 7). These key differences between Cn2 and C113 could help to explain  
5 the lack of interaction between scFv LR and toxin C113.

6 Lior Cohen et al (Cohen et al., 2005) while describing the common features in the  
7 functional surface of scorpion  $\beta$ -toxins highlighted the role of some hydrophobic amino  
8 acids of the Css4 toxin in the interaction with the sodium channel receptor site 4. Some of  
9 these residues are conserved in the hydrophobic surfaces of C113, Cn2 and Css2 as shown  
10 Figure 6. The largest hydrophobic patch is formed by the amino acids Ala17, Leu19 and  
11 Phe44, which are conserved in the three toxins. This hydrophobic patch is situated in the  
12 loop preceding the helix. The two amino acids Ala17 and Leu19 are also conserved within  
13 a hydrophobic patch in Css4 which was demonstrated, introducing some point mutations,  
14 that this toxin segment is important for the Css4 function. Another small hydrophobic patch  
15 is formed by the amino acid Val26 (Leu26 for Cn2 and Css2) which is conserved in the  
16 three toxins and is located on one side of the helix. Finally, there is a third hydrophobic  
17 patch in C113 formed by Ala45 and Cys65, which is also observed in Cn2 and Css2, but in  
18 these toxins it is formed by Cys12 and Cys65.

19 Relevance of positive residues in the biological activity of the cysteine-stabilized proteins  
20 for their binding to channels has been widely studied (Clairfeuille et al., 2019; Estrada et  
21 al., 2011; Goldstein et al., 1994; Hidalgo and MacKinnon, 1995; Krezel et al., 1995; Loret  
22 et al., 1994; MacHado et al., 2018; Stampe et al., 1994), using different methods like  
23 chemical modifications and mutational analysis (Hidalgo and MacKinnon, 1995; Kharrat et  
24 al., 1990). For that reason, we compared the coulombic surface of C113 with that of other  
25 beta toxins which are highly similar in structure and activity namely Cn2 and Css2 (Figure  
26 7). Several positive patches were observed. The first patch in the C-terminal region  
27 includes Lys63 for the three toxins, Arg64 for Cn2 and C113 and Lys66 for C113.

28 Previously, mutagenesis studies and a neutralizing monoclonal antibody have shown the  
29 relevance of His64 in Nav channel modulation which help to guide the  $\alpha$ -toxin into a stable  
30 binding pose (Clairfeuille et al., 2019). For C113 and Cn2 toxins, in this position, it is filled

1 with an Arg64 which forms a positive patch in C-terminal region with Lys63. In Cn2, this  
2 patch is less conserved and is formed by Lys63 and Pro61.

3 Then, there is a second positive patch formed by the amino acids 30 and 35 that is more or  
4 less conserved in the three toxins considering that there is difference in the amino acid  
5 composition, this patch is situated in the loop  $\alpha$ 1- $\beta$ 2. Finally, the amino acid Lys 8 which  
6 has been shown to play an important role for the interaction with the channel (Clairfeuille  
7 et al., 2019; Fabrichny et al., 2012) in the case of  $\alpha$ -toxin, is conserved in Cn2 and C<sub>ss</sub>2,  
8 whereas it is replaced by a tyrosine followed by a histidine in C<sub>l</sub>13. This leads to the  
9 presence of a third positive patch that is not present in C<sub>l</sub>13 as clearly observed in Figure 4.  
10 It clearly appears that C<sub>l</sub>13 displays the largest negative surface as compared to Cn2 and  
11 C<sub>ss</sub>2.

12 It is important to remember the fact that only 10FG2 single-chain antibody fragment of  
13 human origin is able to completely neutralize the two  $\beta$ -toxins C<sub>l</sub>11 and C<sub>l</sub>12, (Riaño-  
14 Umbarila et al., 2019) and that a mixture LR and 10FG2 antibody fragments are not  
15 capable to fully protect against the entire soluble venom of *C. limpidus*, contrary to what it  
16 was shown with toxin Cn2 of *C. noxius*. For this reason the minor component C<sub>l</sub>13 was  
17 isolated, sequenced and physiologically characterized (Olamendi-Portugal et al., 2017). It is  
18 very toxic to mice. The residue Glu15 known to have a crucial role in the action of  $\beta$ -toxins  
19 in term of toxicity (Izhar et al., 2004; Schiavon et al., 2012) is replaced here by a threonine.  
20 C<sub>l</sub>13 is one of the most toxic components that we have studied together with Cn2, which  
21 suggests that there are other residues in the toxin that contribute to the binding and  
22 alteration of the functioning of the above mentioned sodium channels.

23 The study described here shows that the three-dimensional structure of C<sub>l</sub>13 is very similar  
24 to that of Cn2 and C<sub>ss</sub>2 and therefore is likely to be similar to that of C<sub>l</sub>11 and C<sub>l</sub>12 taking  
25 into account the high sequence similarity among these toxins, although the 3D structures of  
26 these two last toxins are not known yet (Figure 4). As reported earlier (Olamendi-Portugal  
27 et al., 2017), the three stretches namely positions 7-9, 30-38 and 62-66, that have been  
28 reported to be different for C<sub>l</sub>13 as compared to the two toxins C<sub>l</sub>11 and C<sub>l</sub>12, might be  
29 responsible for the lack of its interaction with the single chain neutralizing antibodies. In  
30 previous studies of the 3D structure of the ternary complex of the scFv LR, Cn2 and the

1 predecessor scFv of 10FG2 (RU1), it was found that the core of the binding site of scFv LR  
2 is located near the N-terminus of the  $\alpha$ -helix's region of toxin Cn2 whereas that of scFv  
3 RU1 is located near the corresponding C-terminus(Riaño-Umbarila et al., 2016).

4 The alignment shown in figure 4B highlights the amino acid residues recognized in Cn2 by  
5 scFv LR in red and the ones recognized by scFv 10FG2 in blue. In C113 toxin, the amino  
6 acid residues that differ between Cn2 and C113 are highlighted in bold with respect to the  
7 sequence of the Cn2 toxin, Figure 4B. These differences coincide with important anchor  
8 sites of the LR scFv in the Cn2 toxin, since the different contacts formed with Glu15 (a  
9 saline bridge with His35 of the VH domain of the scFv, hydrogen bonds with Ala33,  
10 Gly102, van der Waals contacts with A33H, G99H, V101H in LR) (Canul-Tec et al., 2011).  
11 In the same way, scFv 10FG2 has a very important anchorage with residues Gln31 and  
12 Glu32 of Cn2 (Riaño-Umbarila et al., 2019), which are different in C113 (Leu31 and  
13 Arg31) indicating that these interactions could not be established with toxin C113.

#### 14 **5. Concluding remarks**

15 Having assigned all protons chemical shifts and also most of carbon and nitrogen  
16 chemical shifts for C113 at natural abundance, its NMR solution structure was solved  
17 showing a cysteine-stabilized  $\alpha/\beta$  (CS $\alpha/\beta$ ) motif commonly found in sodium channel  $\beta$ -  
18 toxins. The structural comparison analysis shows that the three-scorpion sodium  $\beta$  toxins  
19 active on mammals share a similar hydrophobic surface and some conserved positive  
20 regions, but also a large negative region for C113 which suggest that the activity of these  
21 disulfide-stabilized proteins is regulated by different interaction interfaces. Indeed, the three  
22 stretches already pointed out as well as the nature of residue at position 15, which in C113 is  
23 a Thr whereas in most of the others is Glu, which might be responsible for the lack of  
24 interaction of C113 toxin with LR. The changes in positions 30, 31 and 32 do not permit the  
25 interaction with 10FG2 and as a consequence, the null neutralization of C113 and the  
26 deficient neutralization of the *Centruroides limpidus* whole venom.

#### 27 **6. Declaration of interest**

28 The authors declare that they have not known competing financial interests or personal  
29 relationships that could have appeared to influence the work reported in this paper.

## 1 7. Acknowledgements

2 The authors acknowledge Dr. Fernando Z. Zamudio for the service of determining the  
3 Edman degradation and mass spectrometry data of this manuscript. The work in Paris was  
4 supported by fund from the Pasteur Institute and the *Centre National de la Recherche*  
5 *Scientifique* (UMR 3528). The 800 MHz NMR spectrometer of the Institut Pasteur was  
6 partially funded by the *Région Ile de France* (SESAME 2014 NMRCHR grant no  
7 4014526). Partially supported by grant FORDECYT 303045 from *Consejo Nacional de*  
8 *Ciencia y Tecnología* to BB and LDP; also, *Dirección General del Personal Académico*  
9 UNAM IN210319 and *Dirección General de Cómputo y de Tecnologías de la Información*  
10 *y Comunicación*, Supercomputing Project LANCAD-UNAM-DGTIC-145 given to FRP.

## 11 8. Bibliography

- 12 Alagón, A.C., Guzmán, H.S., Martín, B.M., Ramírez, A.N., Carbone, E., Possani, L.D., 1988. Isolation  
13 and characterization of two toxins from the Mexican scorpion *Centruroides limpidus limpidus*  
14 Karsch. *Comp. Biochem. Physiol. B.* 89, 153–61. [https://doi.org/10.1016/0305-](https://doi.org/10.1016/0305-0491(88)90277-5)  
15 [0491\(88\)90277-5](https://doi.org/10.1016/0305-0491(88)90277-5)
- 16 Bax, A., Davis, D.G., 1985. MLEV-17-based two-dimensional homonuclear magnetization transfer  
17 spectroscopy. *J. Magn. Reson.* 65, 355–360. [https://doi.org/10.1016/0022-2364\(85\)90018-6](https://doi.org/10.1016/0022-2364(85)90018-6)
- 18 Canul-Tec, J.C., Riaño-Umbarila, L., Rudiño-Piñera, E., Becerril, B., Possani, L.D., Torres-Larios, A.,  
19 2011. Structural basis of neutralization of the major toxic component from the scorpion  
20 *Centruroides noxius* Hoffmann by a human-derived single-chain antibody fragment. *J. Biol.*  
21 *Chem.* 286, 20892–20900. <https://doi.org/10.1074/jbc.M111.238410>
- 22 Chippaux, J.P., Goyffon, M., 2008. Epidemiology of scorpionism: A global appraisal. *Acta Trop.*  
23 <https://doi.org/10.1016/j.actatropica.2008.05.021>
- 24 Cid-Uribe, J.I., Meneses, E.P., Batista, C.V.F., Ortiz, E., Possani, L.D., 2019. Dissecting toxicity: The  
25 venom gland transcriptome and the venom proteome of the highly venomous scorpion  
26 *centruroides limpidus* (Karsch, 1879). *Toxins* (Basel). 11.  
27 <https://doi.org/10.3390/toxins11050247>
- 28 Clairfeuille, T., Cloake, A., Infield, D.T., Llongueras, J.P., Arthur, C.P., Li, Z.R., Jian, Y., Martin-  
29 Eauclaire, M.F., Bougis, P.E., Ciferri, C., Ahern, C.A., Bosmans, F., Hackos, D.H., Rohou, A.,  
30 Payandeh, J., 2019. Structural basis of a-scorpion toxin action on Na<sup>v</sup> channels. *Science* (80-  
31 ). 363, 1–25. <https://doi.org/10.1126/science.aav8573>
- 32 Cohen, L., Karbat, I., Gilles, N., Ilan, N., Benveniste, M., Gordon, D., Gurevitz, M., 2005. Common  
33 features in the functional surface of scorpion  $\beta$ -toxins and elements that confer specificity for  
34 insect and mammalian voltage-gated sodium channels. *J. Biol. Chem.* 280, 5045–5053.  
35 <https://doi.org/10.1074/jbc.M408427200>

- 1 Dalvit, C., Shapiro, G., Bohlen, J., Parella, T., 1991. Technical aspects of an efficient multiple solvent  
2 suppression pulse sequence. *Magn. Reson. Chem.* 37, 7–14.
- 3 Dehesa-Dávila, M., Ramírez, A.N., Zamudio, F.Z., Gurrola-Briones, G., Liévano, A., Darszon, A.,  
4 Possani, L.D., 1996. Structural and functional comparison of toxins from the venom of the  
5 scorpions *Centruroides infamatus infamatus*, *Centruroides limpidus limpidus* and  
6 *Centruroides noxius*. *Comp. Biochem. Physiol. - B Biochem. Mol. Biol.* 113, 331–339.  
7 [https://doi.org/10.1016/0305-0491\(95\)02031-4](https://doi.org/10.1016/0305-0491(95)02031-4)
- 8 Delaglio, F., Grzesiek, S., Vuister, G.W., Zhu, G., Pfeifer, J., Bax, A., 1995. NMRPipe: A  
9 multidimensional spectral processing system based on UNIX pipes. *J. Biomol. NMR* 6, 277–  
10 293. <https://doi.org/10.1007/BF00197809>
- 11 Delrioportilla, F., Blechta, V., Freeman, R., 1994. Measurement of Poorly Resolved Splittings by J  
12 Doubling in the Frequency Domain. *J. Magn. Reson. Ser. A.*  
13 <https://doi.org/10.1006/jmra.1994.1238>
- 14 Downing, A.K., Güntert, P., 2004. Automated NMR Structure Calculation With CYANA. *Protein*  
15 *NMR Tech.* 278, 353–378. <https://doi.org/10.1385/1-59259-809-9:353>
- 16 Dyson, H.J., Rance, M., Houghten, R.A., Lerner, R.A., Wright, P.E., 1988. Folding of immunogenic  
17 peptide fragments of proteins in water solution. I. Sequence requirements for the formation  
18 of a reverse turn. *J. Mol. Biol.* 201, 161–200. [https://doi.org/10.1016/0022-2836\(88\)90446-9](https://doi.org/10.1016/0022-2836(88)90446-9)
- 19 Estrada, G., Restano-Cassulini, R., Ortiz, E., Possani, L.D., Corzo, G., 2011. Addition of positive  
20 charges at the C-terminal peptide region of CsslI, a mammalian scorpion peptide toxin,  
21 improves its affinity for sodium channels Nav1.6. *Peptides* 32, 75–79.  
22 <https://doi.org/10.1016/j.peptides.2010.11.001>
- 23 Fabrichny, I.P., Mondielli, G., Conrod, S., Martin-Eauclaire, M.F., Bourne, Y., Marchot, P., 2012.  
24 Structural insights into antibody sequestering and neutralizing of Na<sup>+</sup> channel  $\alpha$ -type  
25 modulator from old world scorpion venom. *J. Biol. Chem.* 287, 14136–14148.  
26 <https://doi.org/10.1074/jbc.M111.315382>
- 27 Garza-García, A., Ponzanelli-Velázquez, G., del Río-Portilla F, 2001. Deconvolution and  
28 measurement of spin-spin splittings by modified J doubling in the frequency domain. *J. Magn.*  
29 *Reson.* 148, 214–219. <https://doi.org/10.1006/jmre.2000.2235>
- 30 Goldstein, S.A.N., Pheasant, D.J., Miller, C., 1994. The charybdotoxin receptor of a Shaker K<sup>+</sup>  
31 channel: Peptide and channel residues mediating molecular recognition. *Neuron* 12, 1377–  
32 1388. [https://doi.org/10.1016/0896-6273\(94\)90452-9](https://doi.org/10.1016/0896-6273(94)90452-9)
- 33 González-Santillán, E., Possani, L.D., 2018. North American scorpion species of public health  
34 importance with a reappraisal of historical epidemiology. *Acta Trop.* 187, 264–274.  
35 <https://doi.org/10.1016/j.actatropica.2018.08.002>
- 36 Griesinger, C., Otting, G., Wüthrich, K., Ernst, R.R., 1988. Clean tocsy for 1H spin system  
37 identification in macromolecules. *J. Am. Chem. Soc.* 110, 7870–7872.  
38 <https://doi.org/10.1021/ja00231a044>
- 39 Gurrola, G.B., Hernández-López, R.A., Rodríguez De La Vega, R.C., Varga, Z., Batista, C.V.F., Salas-

- 1 Castillo, S.P., Panyi, G., Del Río-Portilla, F., Possani, L.D., 2012. Structure, function, and  
2 chemical synthesis of Vaejovis mexicanus peptide 24: A novel potent blocker of Kv1.3  
3 potassium channels of human T lymphocytes. *Biochemistry* 51, 4049–4061.
- 4 Hidalgo, P., MacKinnon, R., 1995. Revealing the architecture of a K<sup>+</sup> channel pore through mutant  
5 cycles with a peptide inhibitor. *Science* (80-. ). 268, 307–310.  
6 <https://doi.org/10.1126/science.7716527>
- 7 Hwang, T.L., Shaka, A.J., 1995. Water Suppression That Works. Excitation Sculpting Using Arbitrary  
8 Wave-Forms and Pulsed-Field Gradients. *J. Magn. Reson. - Ser. A* 112, 275–279.  
9 <https://doi.org/10.1006/jmra.1995.1047>
- 10 Izhar, K., Lior, C., Nicolas, G., Dalia, G., Michael, G., 2004. Conversion of a scorpion toxin agonist  
11 into an antagonist highlights an acidic residue involved in voltage sensor trapping during  
12 activation of neuronal Na<sup>+</sup> channels. *FASEB J.* 18, 683–689. [https://doi.org/10.1096/fj.03-](https://doi.org/10.1096/fj.03-0733com)  
13 [0733com](https://doi.org/10.1096/fj.03-0733com)
- 14 Keller, R., 2004. The computer aided resonance assignment tutorial, Goldau, Switzerland: Cantina  
15 Verlag.
- 16 Kharrat, R., Darbon, H., Granier, C., Rochat, H., 1990. Structure-activity relationships of scorpion  $\alpha$ -  
17 neurotoxins: Contribution of arginine residues. *Toxicon* 28, 509–523.  
18 [https://doi.org/10.1016/0041-0101\(90\)90295-I](https://doi.org/10.1016/0041-0101(90)90295-I)
- 19 Krezel, A.M., Kasibhatla, C., Hidalgo, P., Mackinnon, R., Wagner, G., 1995. Solution structure of the  
20 potassium channel inhibitor agitoxin 2: Caliper for probing channel geometry. *Protein Sci.* 4,  
21 1478–1489. <https://doi.org/10.1002/pro.5560040805>
- 22 Lebreton, F., Delepierre, M., Ramírez, A.N., Balderas, C., Possani, L.D., 1994. Primary and NMR  
23 Three-Dimensional Structure Determination of a Novel Crustacean Toxin from the Venom of  
24 the Scorpion *Centruroides limpidus limpidus* Karsch. *Biochemistry* 33, 11135–11149.  
25 <https://doi.org/10.1021/bi00203a010>
- 26 Lee, W., Tonelli, M., Markley, J.L., 2015. NMRFAM-SPARKY: Enhanced software for biomolecular  
27 NMR spectroscopy. *Bioinformatics* 31, 1325–1327.  
28 <https://doi.org/10.1093/bioinformatics/btu830>
- 29 Levitt, M.H., Freeman, R., Frenkiel, T., 1982. Broadband heteronuclear decoupling. *J. Magn. Reson.*  
30 47, 328–330. [https://doi.org/10.1016/0022-2364\(82\)90124-X](https://doi.org/10.1016/0022-2364(82)90124-X)
- 31 Loret, E.P., Soto Del Valle, R.M., Mansuelle, P., Sampieri, F., Rochat, H., 1994. Positively charged  
32 amino acid residues located similarly in sea anemone and scorpion toxins. *J. Biol. Chem.* 269,  
33 16785–16788.
- 34 MacHado, L.E.S.F., De Paula, V.S., Pustovalova, Y., Bezsonova, I., Valente, A.P., Korzhnev, D.M.,  
35 Almeida, F.C.L., 2018. Conformational Dynamics of a Cysteine-Stabilized Plant Defensin  
36 Reveals an Evolutionary Mechanism to Expose Hydrophobic Residues. *Biochemistry* 57,  
37 5797–5806. <https://doi.org/10.1021/acs.biochem.8b00753>
- 38 Medvedeva, S., Simorre, J.P., Brutscher, B., Guerlesquin, F., Marion, D., 1993. Extensive 1H NMR  
39 resonance assignment of proteins using natural abundance gradient-enhanced 13C-1H

1 correlation spectroscopy. FEBS Lett. 333, 251–256. [https://doi.org/10.1016/0014-](https://doi.org/10.1016/0014-5793(93)80664-G)  
2 5793(93)80664-G

3 Notredame C, Higgins DG, H.J., 2000. T-Coffee: a novel method for fast and accurate multiple  
4 sequence alignment. *J Mol Biol* 17, 302:205.

5 Olamendi-Portugal, T., Restano-Cassulini, R., Riaño-Umbarila, L., Becerril, B., Possani, L.D., 2017.  
6 Functional and immuno-reactive characterization of a previously undescribed peptide from  
7 the venom of the scorpion *Centruroides limpidus*. *Peptides* 87, 34–40.  
8 <https://doi.org/10.1016/j.peptides.2016.11.008>

9 Pettersen EF, Goddard TD, Huang CC, Couch GS, Greenblatt DM, Meng EC, F.T.J., 2004. UCSF  
10 Chimera--a visualization system for exploratory research and analysis. *Comput Chem.* 25,  
11 1605-1612.

12 Piantini, U., Sørensen, O.W., Ernst, R.R., 1982. Multiple Quantum Filters for Elucidating NMR  
13 Coupling Networks. *J. Am. Chem. Soc.* 104, 6800–6801. <https://doi.org/10.1021/ja00388a062>

14 Pintar, A., Possani, L.D., Delepierre, M., 1999. Solution structure of toxin 2 from *Centruroides*  
15 *noxius* Hoffmann, a  $\beta$ -scorpion neurotoxin acting on sodium channels. *J. Mol. Biol.* 287, 359–  
16 367. <https://doi.org/10.1006/jmbi.1999.2611>

17 Possani, L.D., Becerril, B., Delepierre, M., Tytgat, J., 1999. Scorpion toxins specific for Na<sup>+</sup>-  
18 channels. *Eur. J. Biochem.* <https://doi.org/10.1046/j.1432-1327.1999.00625.x>

19 Ramírez, A.N., Martín, B.M., Gurrola, G.B., Possani, L.D., 1994. Isolation and characterization of a  
20 novel toxin from the venom of the scorpion *Centruroides limpidus limpidus* Karsch. *Toxicon*  
21 32, 479–490. [https://doi.org/10.1016/0041-0101\(94\)90300-X](https://doi.org/10.1016/0041-0101(94)90300-X)

22 Rance, M., Sørensen, O.W., Bodenhausen, G., Wagner, G., Ernst, R.R., Wüthrich, K., 1983.  
23 Improved spectral resolution in COSY 1H NMR spectra of proteins via double quantum  
24 filtering. *Biochem. Biophys. Res. Commun.* 117, 479–485. [https://doi.org/10.1016/0006-](https://doi.org/10.1016/0006-291X(83)91225-1)  
25 291X(83)91225-1

26 Riaño-Umbarila, L., Contreras-Ferrat, G., Olamendi-Portugal, T., Morelos-Juárez, C., Corzo, G.,  
27 Possani, L.D., Becerril, B., 2011. Exploiting cross-reactivity to neutralize two different  
28 scorpion venoms with one single chain antibody fragment. *J. Biol. Chem.* 286, 6143–6151.  
29 <https://doi.org/10.1074/jbc.M110.189175>

30 Riaño-Umbarila, L., Gómez-Ramírez, I. V., Ledezma-Candanoza, L.M., Olamendi-Portugal, T.,  
31 Rodríguez-Rodríguez, E.R., Fernández-Taboada, G., Possani, L.D., Becerril, B., 2019.  
32 Generation of a broadly cross-neutralizing antibody fragment against several mexican  
33 scorpion venoms. *Toxins (Basel)*. 11. <https://doi.org/10.3390/toxins11010032>

34 Riaño-Umbarila, L., Ledezma-Candanoza, L.M., Serrano-Posada, H., Fernández-Taboada, G.,  
35 Olamendi-Portugal, T., Rojas-Trejo, S., Gómez-Ramírez, I. V., Rudiño-Piñera, E., Possani, L.D.,  
36 Becerril, B., 2016. Optimal neutralization of *Centruroides noxius* venom is understood  
37 through a structural complex between two antibody fragments and the Cn2 toxin. *J. Biol.*  
38 *Chem.* 291, 1619–1630. <https://doi.org/10.1074/jbc.M115.685297>

39 Riaño-Umbarila, L., Olamendi-Portugal, T., Morelos-Juárez, C., Gurrola, G.B., Possani, L.D., Becerril,

1 B., 2013. A novel human recombinant antibody fragment capable of neutralizing Mexican  
2 scorpion toxins. *Toxicon* 76, 370–6. <https://doi.org/10.1016/j.toxicon.2013.09.016>

3 Santibáñez-López, C.E., Francke, O.F., Ureta, C., Possani, L.D., 2015. Scorpions from Mexico: From  
4 species diversity to venom complexity. *Toxins* (Basel).  
5 <https://doi.org/10.3390/toxins8010002>

6 Saucedo, A.L., Del Rio-Portilla, F., Picco, C., Estrada, G., Prestipino, G., Possani, L.D., Delepiere, M.,  
7 Corzo, G., 2012. Solution structure of native and recombinant expressed toxin CsslI from the  
8 venom of the scorpion *Centruroides suffusus suffusus*, and their effects on Nav1.5 Sodium  
9 channels. *Biochim. Biophys. Acta - Proteins Proteomics* 1824, 478–487.

10 Schiavon, E., Pedraza-Escalona, M., Gurrola, G.B., Olamendi-Portugal, T., Corzo, G., Wanke, E.,  
11 Possani, L.D., 2012. Negative-shift activation, current reduction and resurgent currents  
12 induced by  $\beta$ -toxins from *Centruroides* scorpions in sodium channels. *Toxicon* 59, 283–293.  
13 <https://doi.org/10.1016/j.toxicon.2011.12.003>

14 Schiavon, E., Sacco, T., Cassulini, R.R., Gurrola, G., Tempia, F., Possani, L.D., Wanke, E., 2006.  
15 Resurgent current and voltage sensor trapping enhanced activation by a  $\beta$ -scorpion toxin  
16 solely in Na v1.6 channel: Significance in mice Purkinje neurons. *J. Biol. Chem.* 281, 20326–  
17 20337. <https://doi.org/10.1074/jbc.M600565200>

18 Secretaria de Salud, 2015. Casos por entidad federativa de enfermedades no transmisibles hasta la  
19 semana epidemiológica, in: V.D.B.Epidemiologia (Ed.), B. d. V. Epidemiologica. Mexico, p. 52.

20 Shen, Y., Bax, A., 2013. Protein backbone and sidechain torsion angles predicted from NMR  
21 chemical shifts using artificial neural networks. *J. Biomol. NMR* 56, 227–241.  
22 <https://doi.org/10.1007/s10858-013-9741-y>

23 Stampe, P., Kolmakova-Partensky, L., Miller, C., 1994. Intimations of K<sup>+</sup> Channel Structure from a  
24 Complete Functional Map of the Molecular Surface of Charybdotoxin. *Biochemistry* 33, 443–  
25 450. <https://doi.org/10.1021/bi00168a008>

26 States, D.J., Haberkorn, R.A., Ruben, D.J., 1982. A two-dimensional nuclear overhauser experiment  
27 with pure absorption phase in four quadrants. *J. Magn. Reson.* 48, 286–292.  
28 [https://doi.org/10.1016/0022-2364\(82\)90279-7](https://doi.org/10.1016/0022-2364(82)90279-7)

29 Wagner, G., Zuiderweg, E.R., 1983. Two-dimensional double quantum <sup>1</sup>H NMR spectroscopy of  
30 proteins. *Biochem. Biophys. Res. Commun.* 113, 854–60. [https://doi.org/10.1016/0006-  
31 291x\(83\)91077-x](https://doi.org/10.1016/0006-291x(83)91077-x)

32 Wüthrich, K., 1986. NMR with Proteins and Nucleic Acids. *Europhys. News.*  
33 <https://doi.org/10.1051/eprn/19861701011>

34 Xu, J., Zhang, Y., 2010. How significant is a protein structure similarity with TM-score = 0.5?  
35 *Bioinformatics* 26, 889–895. <https://doi.org/10.1093/bioinformatics/btq066>

36



